Towards MRI Differentiation of Recurring Tumor from Delayed Radiation Necrosis

Carlos J Perez-Torres[1], John A Engelbach[1], Jeremy Cates[2], Dinesh K Thotala[2], Robert E Drzymala[2], Joseph JH Ackerman[1,3], and Joel R Garbow[1]
[1]*Department of Radiology, Washington University in Saint Louis, Saint Louis, Missouri, United States,* [2]*Department of Radiation Oncology, Washington University in Saint Louis, Saint Louis, Missouri, United States,* [3]*Department of Chemistry, Washington University in Saint Louis, Saint Louis, Missouri, United States*

Target audience: Clinicians, biologists, and imaging scientists interested in cancer and its treatment with radiation.

Purpose: Accurate diagnosis is essential for proper treatment decisions. Standard anatomical MRI is incapable of differentiating recurring tumor from delayed radiation necrosis, as both lesions are hyperintense in post-contrast T1- and T2-weighted images. Further studies are therefore necessary to accurately identify a robust imaging paradigm that can differentially diagnose these pathologies. Our group has developed a unilateral animal model of delayed radiation necrosis that recapitulates the histological progression seen in patients and has studied it via anatomical MRI[1]. The work presented here further investigates this model with more advanced MRI methodologies, including diffusion-weighted imaging (DWI) and magnetization transfer contrast (MTC). Since the ultimate goal of the project is to differentiate necrosis from tumor, an orthotopic brain tumor model was also examined via the same MRI methodologies.

Methods: *Mouse Models:* All experiments were approved by the Washington University Division of Comparative Medicine and were performed on 8-9 week old female BALB/c mice (Harlan Laboratories, Indianapolis, Indiana). For the radiation necrosis model, mice were irradiated with the Leksell Gamma Knife Perfexion (Elekta, Stockholm, Sweden) with a single 50-Gy dose (50% isodose). Irradiation was focused on the cortex of the left hemisphere ~ 3 mm posterior to bregma. For the tumor model, mice were secured in a stereotactic frame and anesthetized with isoflurane. DBT cells (~10,000 in 10 µl) were injected over 3 minutes at a site 1 mm anterior and to the left of bregma and 2 mm below the cortical surface.

Imaging: Mice were anesthetized with isoflurane and restrained via a 3-point head holder. Images were acquired with a 4.7 T small-animal Agilent/Varian DirectDrive scanner using an actively decoupled volume (transmit) and 1.5 cm surface coil (receive). Several datasets were acquired for each animal, including: MTC, DWI, and anatomical T2 and post-contrast T1. All data were collected with a field of view of 15 x 15 mm^2 and 15 slices, thickness = 0.5 mm. For MTC, images were acquired with and without the application of a 10 ms, 500º saturation pulse applied at a frequency offset +10 ppm from the water resonance. The Magnetization Transfer Ratio (MTR) was calculated as the percent of signal lost due to the saturation pulse. For DWI, the isotropic apparent diffusion coefficient (ADCi) was calculated as the average of three separate diffusion datasets, acquired with diffusion encoding along 3 orthogonal directions, with a b-value of 1000 s/mm^2. ROIs were drawn on the anatomical images and then applied to the MTR and ADCi images. Values were normalized relative to the contralateral (normal) side of the brain in each mouse to produce rMTR and rADCi. For each model, a total of 4 mice were studied and values are presented as mean ± standard deviation. P-values presented are from Student's t-test.

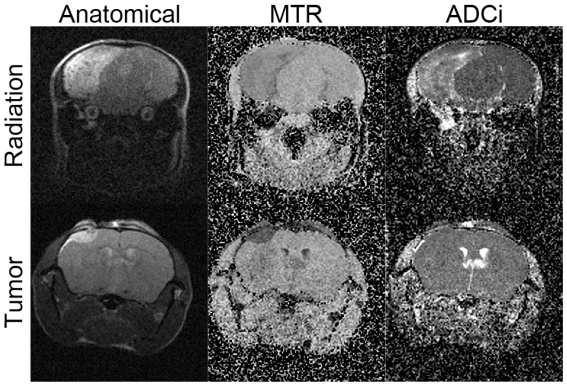

Results: Results for a representative mouse six weeks after irradiation (top row) or ten days after tumor injection (bottom row) are shown in the figure. As previously reported, both lesion types are hyperintense in T2-weighted anatomical scans (first column). Both lesions also show a hypointense pattern in the MTR (second column). The necrosis model showed a rMTR of 0.90±0.02 while the tumor model showed a rMTR of 0.67±0.07 ($P<0.001$). Differences in ADCi (third column) are observed between tumor and necrosis. The ADCi of the necrotic region shows diffuse enhancement (rADCi of 1.27±0.12), while the tumor ADCi is predominantly normointense (rADCi of 1.08±0.09) relative to the surrounding healthy brain tissue ($P<0.05$).

Discussion: The primary goal of this project is to develop a robust imaging paradigm capable of distinguishing between radiation necrosis and tumor recurrence. Both tumor and necrosis showed decreases in rMTR, with the MT effect being stronger for tumor than radiation necrosis. The ADCi for tumor was similar to that of healthy brain, while ADCi was elevated in necrosis. Because tumor ADC has been shown to be variable in humans[2], these results should be validated with other tumor models. It will also be important to evaluate changes in both models longitudinally. These changes will likely be more meaningful and more robust than single time-point measurements. A prior study explored both MTR and ADC in a different radiation necrosis model[3], but did not compare the necrosis to a tumor model. Our ADC results are consistent with this previous report, but, unlike the earlier study, we were able to identify the necrosis on the MTR, a difference likely due to a difference in saturation pulse power.

Conclusion: MTR and ADC provide metrics distinguishing tumor vs. radiation necrosis. A multi-contrast MRI approach that includes both modalities holds promise for differentiating between these pathologies.

References: 1. Jost SC, Hope A, Kiehl E, Perry A, Travers S, Garbow JR. A Novel Murine Model for Localized Radiation Necrosis and its Characterization Using Advanced Magnetic Resonance Imaging. *Int J Radiat Oncol Biol Phys.* 2009;75(2):527–533.2. Kono K, Inoue Y, Nakayama K, et al. The Role of Diffusion-weighted Imaging in Patients with Brain Tumors. *AJNR Am J Neuroradiol*. 2001;22(6):1081–1088.3. Wang S, Tryggestad E, Zhou T, et al. Assessment of MRI Parameters as Imaging Biomarkers for Radiation Necrosis in the Rat Brain. *Int J Radiat Oncol Biol Phys.* 2012;83(3):e431–e436.